PCCP

Accepted Manuscript

ROYAL SOCIETY OF CHEMISTRY

www.rsc.org/pccp

Adsorption properties of trifluoroacetic acid on anatase (101) and (001) surfaces: A density functional theory study

Oriol Lamiel Garcia,[1] Daniel Fernandez-Hevia,[2,3] Amador C. Caballero,[4] Francesc Illas[1*]

[1)] *Departament de Química Física &Institut de Química Teòrica i Computacional (IQTCUB), Universitat de Barcelona, C/ Martí i Franquès 1, E-08028 Barcelona, Spain*

[2)] *INAEL Electrical Systems S.A., C/ Jarama 5, 45007 Toledo, Spain*

[3)] *Departamento de Química, Universidad de Las Palmas de Gran Canaria, Campus Universitario de Tafira, 35017 Las Palmas de Gran Canaria, Spain*

[4)] *Department of Electroceramics, Instituto de Cerámica y Vidrio (CSIC), Kelsen 5, 28049, Madrid, Spain*

Abstract.-

The interaction of trifuoroacetic acid with the anatase TiO_2(101) and TiO_2(001) surfaces has been studied by means of periodic density functional theory based calculations. On the former, the interaction is weak with the adsorbed molecules in a configuration almost indistinguishable from the gas phase structure. On the latter, the interaction is very strong; the molecule adsorbs as trifluoroacetate and releases a proton that binds an oxygen surface atom with a significant distortion of the substrate. The difference in adsorption mode and strength can be understood from the different structural features of both surfaces and provides arguments to the role of trifluoroacetic as morphological control agent in the solvothermal synthesis of TiO_2 nanoparticles with predominant (001) facets. This, in turn, has a very significant impact in industrial production strategies of value-added TiO_2 for photocatalytic applications. Analysis of calculated core level binding energies for F(1s) confirms the experimental assignment to F at the surface as F^- at Ti surface sites and to F in $–CF_3$ groups of the adsorbed molecule.

* Corresponding author. Tel: +34 934 021 229. e-mail: francesc.illas@ub.edu

Introduction

Photocatalysis constitutes a very active field of research due to its implications in environmental chemistry,[1,2] hydrogen production,[3,4] self-cleaning surfaces,[5] self-sterilizing surfaces[6] and water cleaning technologies.[7] Among the different materials scrutinized as possible photocatalysts, titanium dioxide (TiO_2) continues to be one of the main key players.[2,4,7-9] TiO_2 exhibits three stable polymorphs namely anatase, rutile and brookite among which anatase exhibits the highest activity and is present in most of the existing photocatalysts based on this material. This is the case of the well-known commercial Degussa P25 (Evonik) catalyst often used as a standard even if its exact composition remains a matter of controversy.[10] Nevertheless, the excessively large bandgap of the bulk forms of TiO_2 (rutile ≈ 3 eV and anatase ≈ 3.2 eV) severely limits its efficient use for photocatalysis under visible light. Several strategies have been proposed to decrease the bandgap of anatase involving new synthetic processes aimed at introducing doping either with non-metals, metals or simply introducing defects.[11,12]The case of doping with nitrogen is very illustrative as it raised enormous expectation; over 5.000 citations have followed its publications in 2001 by Asahi et al.[13] However, in spite of initial evidence, the photocatalytic reaction rates are still low. More importantly, the detailed origin of photocatalysis over visible-light-activated N-doped TiO_2 is still a matter of considerable controversy.[14,15]Nevertheless, in spite of all these efforts, photocatalyst working under visible sunlight with activity higher than TiO_2 powders under ultraviolet light have not been yet developed.[16]

A different approach to enhance the photocatalytic activity of TiO_2 under the visible consists in controlling morphology and size of the nanoparticles constituting the TiO_2 based powders such as the above mentioned Degussa P25 (Evonik). In this respect, the seminal work of Yang et al.[17]showing that adsorbed F stabilizes the reactive (001) surface of TiO_2 anatase in detriment of the most stable and abundant but less active (101) surface represents a major breakthrough. TiO_2 anatase single crystal mesoparticles with controlled size, well-defined polyhedral facets,[18,19] and high-level photocatalytic activities have been synthetized in the past few years. The enormous degree of experimental control achieved in the synthesis of tailored TiO_2 nanoparticles with either anatase or rutile crystal structure is well-describe in the recent review by Liu et al.[20] Nevertheless, it is worth pointing out that a clear cut relationship with particle morphology and photocatalytic activity does not so far exist. Yet, this understanding is

critical in order to promote the development of large-scale production facilities that can produce a low-cost/high-efficiency TiO_2-based material and create a competitive advantage in the industry by leveraging the nanoscale morphology control. Note, for instance, that high photocatalytic activity has also been reported as well for TiO_2 nanoparticles with dominant (111) facets.[21]

The synthesis of TiO_2 nanoparticles with abundant (001) surfaces often involves hydrothermal processes with hydrofluoric acid (HF) as fluorine source. The presence of fluorine increases the surface free energy of the most stable (101) face and decreases the surface free energy of the initially less stable (001).[22] The problem with the use of HF is its high toxicity, high reactivity and corrosive behavior. Recently, trifluoroacetic acid (TFAA) has proven to be efficient in obtaining TiO_2 with a large amount of (001) surfaces and resulted in samples with enhanced photoactivity.[23] Moreover, the use of TFAA enormously reduces the presence of water in the reaction medium allowing for a better control. The experiments of Calatayud et al. suggest that TFAA acts as fluorine source. Moreover, analysis of X-Ray Photoemission Spectra (XPS) for the F(1s) core suggest that F is simultaneously present as direct adsorbate (Ti-F) and also as part of the CF3COO moiety (C-F). Infrared and Raman spectra suggest that TFAA species are adsorbed through the O atoms in a bidentate mode, either bridging or chelating. The stabilization of the (001) facets may be attributed to the presence of adsorbed atomic F released under the semi-solvothermal reaction or to the presence of the carboxylic group which are also known to stabilize the (001) facet.[24]

In order to further understand the interactions between TFAA and the TiO_2 surfaces and to shed light into the role of TFAA on stabilizing the reactive (001) facets, a series of systematic periodic density functional theory based calculations have been carried aimed at disclosing the preferential adsorption mode at each surface and to further confirm the assignment of XPS peaks corresponding to the F(1s) core level binding energies. The present results fully confirm the experimental assignment and suggest that the simultaneous presence of TFAA and atomic F at the surface acts in a synergic way with the result of a preferential stabilization of the (001) facets.

Computational details

Periodic density functional theory (DFT) based calculations were performed for suitable surface slab models of the clean TiO_2(001) and TiO_2(101) surfaces as well as for

various adsorption modes of the TFAA molecule. Details regarding the surface models and adsorption modes are described in the next section.

In the present DFT calculations the valence electrons are described with a plane wave basis set with a kinetic energy cutoff of 400 eV for the plane waves, enough to obtain total energies converged up to 1 meV/atom. The effect of the inner cores on the valence electron density is taken into account by means of the projector augmented wave (PAW) method,[25,26]this may be regarded as an all electron approach in which the cores are frozen as in the reference system used to extract the corresponding PAW. The *3p*, *3d* and *4s* (12 electrons) of Ti and *2s* and *2p* electrons of C, O and F (4, 6 and 7 electrons, respectively) are explicitly included in the calculation. Numerical integration in the reciprocal space has been carried out by sampling the Brillouin zone using the Monkhorst–Pack method;[27]in particular a 2×2×1 grid of special *k*-points has been used. The same number of k-points was used for the electronic analysis and for the optimization process. Calculations for the isolated TFAA molecule were carried out at the Γ point. All calculations involve closed shell species and non-magnetic material. Accordingly, the non-spin polarized implementation of the periodic Kohn-Sham formalism was always used. Geometry optimizations regarding relaxation of the surface models without or with TFAA were carried out using analytical gradients a convergence was achieved when forces on the relaxed atoms (see below) are less than $5 \cdot 10^{-3}$eV/Å. The same criterion has been used to optimize the geometry of the isolated TFAA molecule which has been carried out by placing the molecule in a large enough cubic box (15 Å/side,).

The generalized gradient approximation (GGA) in the Perdew–Burke–Ernzerhof (PBE) formulation was used for the electron exchange and correlation contribution to the total energy.[28,29]This type of approach is known to considerably underestimate the band gap of oxides in general and of TiO_2 in particular and is especially problematic in the description of reduced titania.[30] A better description is obtained using either PBE+U or hybrid functionals.[31,32]Nevertheless, one must caution that the choice of the hybrid functional (amount of Fock exchange) is an open issue[33,34] and that the nature of electronic states of reduced anatase is a matter of discussion.[35,36] However, since only stoichiometric models considered here and the main purpose of the present work is to investigate the adsorption properties of TFAA on TiO_2 surfaces, one may consider that the choice of standard PBE is adequate enough. This also implies that dispersion terms

are not taken into account. In the forthcoming discussion we will show that this does not represent a limitation and does not affect the main conclusions.

All calculations were carried out have been carried using the VASP code.[37-39]

Surface Models and bonding modes

The TiO_2 (001) and (101) surfaces have been represented within the repeated slab model using large enough super cells built from lattice parameters optimized consistently with the density functional theory (DFT) based method used. The lattice parameters calculated with the computational setup described in the previous section are $a = b$ =3.806 Å and c= 9.734 which compare rather well with the experimental values ($a = b$ = 3.78 Å and c=9.50 Å)[40] and are similar to values reported in previous work dealing with F adsorption[22] and implantation.[41]These works have shown that these models provide converged results with respect of the slab thickness and vacuum width between the periodically repeated slabs although the presence of TFAA requires some adjustment as explained in detail below.

The anatase TiO_2(001) surface has been represented by a 3×3×9 super cell with dimensions 11.419×11.419×33.877 Å including a vacuum width in the direction perpendicular to the surface plane larger than10 Å between the interleaved slabs. The overall surface model contains 72 TiO_2 units. The position of the atoms in the upper layers was fully relaxed whereas those lying 5 Å below the surface plane were fixed to reproduce the bulk structure. In the case of the anatase TiO_2(101) surface the supercell dimensions are 10.448×11.419×31.528 Å and also include the vacuum width between the interleaved slabs. The slightly different dimensions in the (101) plane arise from the tilted nature of the slab model and do not introduce any spurious effect. The resulting model contains 60 $TiO_2$and the position of the atoms in the outermost layers was fully relaxed whereas atoms below 5 Å were fixed at the bulk structure as in the case of the TiO_2(001) surface model. Here it is worth to point out that the anatase TiO_2(001) surface is known to exhibit reconstruction in ultra-high-vacuum conditions[42] and several models have been proposed.[43] These effects are likely to be suppressed in the solvothermal conditions at which the synthesis takes place. Hence, unreconstructed models are used.

The slab models above described are similar but larger than those used in previous studies regarding F adsorption[22] and implantation.[41] The main difference concerns the number of atomic layers, which is larger here, and the dimension of the cell in the c

direction, which is also larger due to the need to accommodate the TFAA adsorbed molecule while maintaining a large enough vacuum width between the periodically repeated models. A graphical representation of both surface models is reported in Figure 1. To investigate the adsorption mode and adsorption coordination of TFAA on the two surface models several initial geometries have been tested in a systematic way, some representative examples are shown in Figure 2 for the case of the TiO_2(001) surface and further discussed in the next section.

It is worth noting that at the conditions of the semi-solvothermal synthesis,[23] the TFAA may be hydrated with several water molecules even if the presence of water was minimal. Several isomers of hydrated TFAA have been described from experiment[44] or from theoretical calculations.[45,46] However, to better understand the type of interaction of TFFA with the TiO_2 surfaces of interest we considered the isolated molecule without solvating water molecules. We will show that TFAA adsorbs strongly on TiO_2(001) and weakly on TiO_2(101), the energy difference is so large that the conclusions will not be affected when considering the hydrated molecule, in one case the interaction will be still weak and in the other case the interaction with the surface will displace the solvating water molecules. One may also wonder whether the strong acid character of TFAA results in dissociative adsorption and whether the resulting structure resembles that of formic or acetic acid adsorbed on these surfaces.[47-4849] We will show that the strong acid character of TFAA leads to adsorption modes that do not resemble those of formic or acetic acid. In addition, the strong acid character favors dissociative adsorption and this is the final optimized geometry even if the initial geometry always concerns molecular adsorption.

For the final optimized configurations the adsorption energy (E_{ads}) has been calculated as usual as

$$E_{ads} = E_{(surf+TFAA)} - (E_{surf} + E_{TFAA})$$

where $E_{(surf+TFAA)}$ stands for the energy of the slab model plus the TFAA in the final optimized geometry, E_{surf} stands for the energy of the relaxed naked surface and, finally, E_{TFAA} corresponds to the energy of the isolated TFAA molecules obtained as indicated in the previous sections.

In order to further insight into the electronic structure of TFAA adsorbed on the TiO_2 surface of interest, core level binding energy for F(1s) electrons in different

environments were estimated within the initial state approximation and hence estimated directly from the Kohn-Sham (KS) eigenvalues (ε_{KS}) of a particular core state with respect to the Fermi energy. The values thus obtained are generally two small compared to experiment and imply meaningless positive relaxation energy values; the change in the total energy due to the change in electronic density of the core state in response to the core hole. Nevertheless, it has been recently shown that while ε_{KS} cannot be compared to absolute values of the core level binding energy, the differences with respect to a common reference (core level binding energy shifts or $\Delta\varepsilon_{KS}$) are physically meaningful[50,51] thus justifying a common practice (see e.g. Refs. 52, 53).

Results and discussion

Adsorption structure and energy

In order to assess the effect of the TiO_2 surface on the structure of the TFAA it is convenient to analyze first the structure of the isolated molecule. This would also allow us to evaluate the accuracy of the present computational approach, at least for structural parameters. There are very few works reporting the structure of the gas phase TFAA molecule and the only experimental information corresponds to the data obtained from electron diffraction.[54] From the computational point of view, the structure has been studied in the context of accurate pK determination at various theoretical levels.[55] Table 1 reports results for structural parameters obtained in the present work and compares them with those reported at the B3LYP/6-311+G(d,p) and MP2(full)/6-311+G(d,p)and levels of theory by Namazian et al.[55] The analysis of results collected in Table 1 indicates that, not surprisingly, PBE results for distances and angles agree with those obtained using the more sophisticated B3LYP and MP2 approaches and with experiment. In fact, the distances all agree within 0.01 Å and the angles by less than 1 degree.

Let us now consider the case of the adsorbed molecule on the most stable TiO_2(101) surface. The geometry optimization procedure was started from almost all possible coordination modes and orientations of the TFAA molecule to the surface. Thus, orientations with the molecule parallel or perpendicular to the surface were considered and each case initial geometries were tried with the molecule placed above different surface sites. The parallel initial geometry always evolves to a perpendicular one with the O atoms pointing towards the surface. For the perpendicular orientation, the bridge, chelate, and monodentate bonding modes were considered; the orientation with the CF_3-

moiety pointing towards the surface is found to be repulsive. In the bridge, chelate, and monodentate bonding modes the O atoms point towards the surface and directly interacting with the Ti surface atoms. Except for the latter, the final geometry corresponds to a non-dissociative adsorption with a very weak interaction. Figure 3 displays two of the final geometries, in one case the H atom of the TFAA molecule interacts with an O atom of the surface (O_{surf}) whereas in the other case the contact involves the O atom of the TFAA molecules not attached to H and one Ti atom (Ti_{surf}). In both cases, the structure of the adsorbed molecule is almost indistinguishable from that of the gas phase TFAA. This is a clear indication that, in theTiO_2(101) surface, the molecule is physisorbed. This conclusion is reinforced by the calculated values of the adsorption energy since, in spite of the difference of coordination mode, the adsorption energy values are almost identical (E_{ads}~ 0. 35 eV). There are several other similar structures with different coordination but all of them have even lower E_{ads} values. This is characteristic of physisorbed species where the interaction is not directional and the molecular structure is preserved. One can properly argue that the calculated E_{ads} values are too small since the present computational approach does not include dispersion forces. However, while the inclusion of dispersion forces can easily double the E_{ads} calculated value,[56,57] it is very unlikely that dispersion forces will change the bonding mechanism and qualitative picture, the TFAA molecule will be predicted to be molecularly adsorbed.

Interestingly, a completely different picture emerges from the calculations when considering the more reactive anatase TiO_2(001) surface. Here, geometry optimization was also carried out starting from different bonding modes and orientations of the TFAA molecule with respect to the surface. Overall, 15 possible adsorption configurations have been considered which can be mainly divided in three groups according to the bonding modes displayed in Figure 2. Following the strategy used for the TiO_2(101) commented above, different bonding modes were tested, considering different orientations, with the molecule perpendicular to the surface or slightly tilted. Initial geometries where the TFAA molecule was parallel to the surface were also checked and the bonding modes where the fluor atoms where the main contact of the molecule with the surface were also considered. However, in all cases, the most stable configuration corresponds to a situation in which the OH bond dissociates, the H atom binds to one of the O_{surf} atoms which is considerably displaced from the equilibrium position towards the vacuum and the

trifluoroacetate moiety is bonded to the surface directly through two O-Ti_{surf} bonds (Figure 4). For this trifluoroacetate adsorbed structure, the C-O distances are almost equal (Table 1) as expected from symmetry arguments and verified by the gas phase calculations of Namazian et al.[55] The corresponding adsorption energy is very large (E_{ads} = 3.36 eV) indicating a very strong interaction. This is remarkable since this bonding mode involves the deformation of the surface. Note that the cost corresponding to the dissociation of the O-H bond will be largely compensated by the formation of the H-O_{surf} bond. Interestingly, the resulting bridging adsorption mode is in agreement with the suggestion from analysis of the infrared spectra of TFAA on TiO_2 anatase nanoparticles.[23] The particular bonding geometry of the trifluoroacetate moiety on TiO_2(001) explains why a similar structure cannot be stabilized on the TiO_2(101), in the latter surface the O atoms of the TFAA molecule cannot directly interact with the Ti_{surf} atoms which are located slightly below the surface plane. It is worth pointing out that a second rather stable structure is found with E_{ads}= 2.80 eV involving also a bridging type configuration. However, in this second adsorption mode the OH moiety of TFAA is preserved, the second O atom of TFAA binds a Ti_{surf} atom making a first C-O-Ti_{surf} and the bridging mode is completed by pulling one of the O_{surf} atoms so as to build the second C-O_{surf}-Ti_{surf} pillar of the bridge. This type of configuration is, however, less stable and unlikely to be found under ultra-high-vacuum conditions. Nevertheless, this can play a role on the semi solvo-thermal synthesis conditions used by Calatayud et al.[23] and may be the reason why a too high temperature results in nanoparticles with less well-defined facets.

Interpretation of XPS experiments

To complete the discussion we will now focus on the interpretation of the XPS experiments reported by Calatayud et al.[23] These authors find two well separated contributions corresponding to the F(1s) core level binding energies. The first peak appears at 684 eV and is attributed to F species adsorbed above Ti_{surf} sites, the second peak exhibits larger intensity and appears at a rather higher binding energy of 688 eV and is attributed to F atoms on the $–CF_3$ moiety of the TFAA molecule. Both features are relative to C(1s) at 284.6 which was used for calibration. From chemical intuition and as confirmed by previous theoretical calculations, F species at the surface are negatively charged with almost 1e transferred from the substrate.[22] Therefore, charge transfer arguments suggest to assign the peak at lower binding to F^- species above Ti_{surf} sites and

the peak at higher binding energy to F atoms in the $–CF_3$ group. This assignment is fully confirmed by the present DFT based calculations predicting also two main XPS peaks at 655.0 and 657.5eV, respectively. The peak at lower binding energy corresponds to F atoms at the surface precisely above Ti_{surf} sites and the one at higher binding energy corresponds to the F atoms in the $–CF_3$ group. For comparison we have also obtained the F(1s) binding energy corresponding to the F_2 molecule where the F atoms are necessarily neutral. The calculated F(1s) binding energy is much higher,~664 eV, as expected.

At this point, the reader would have noticed that the trends in the calculated core level binding energies commented above agree well with the experimental ones but also that the absolute values are quite different thus severely questioning the validity of the present theoretical predictions. There are several reasons for the discrepancy between experimental and calculated absolute values of the F(1s) binding energies. Some reasons are purely technical and some other have a more fundamental origin.[58,59] Regarding the former, one needs to realize that experimental values are relative to C(1s) centered at 284.6 eV. This is usual convention but note the experiments for the gas phase TFAA molecule report C(1s) binding energies of 296.5 and 299.3 for the C atom in the -COO and $–CF_3$ groups respectively.[60] Within the present approach, the calculated values for the gas phase TFAA molecule are 273.9 and 276.8, the trend is as in the experiment with a difference between the two C(1s) binding energies of 2.8 eV in the experiment and 2.9eV in the calculated values. However, the absolute values are too small and this brings us to the more fundamental reasons for quantitative disagreement. The calculated values correspond to the so-called initial state estimate and here are approximated from the Kohn-Sham orbital energies. This is a common practice, fully justified from at the Hartree-Fock level of theory[58,59] through the Koopman's theorem and assumed to be valid in DFT based calculations, the latter hypothesis being often justified from practical observation.[52,53]We already mentioned that it has been recently shown that Kohn-Sham orbital energies do not provide an estimate of core level binding energies,[50,51] the values thus obtained are too small implying a negative contribution of final state effects, the energy gain due to the relaxation of the electron density in response to the core hole must be necessarily negative. Interestingly, Kohn-Sham orbital energies with respect to a given reference follow the experimental trend, as shown in recent work[50,51] and illustrated here with the example of C(1s) for the TFAA molecule above, and this is the origin of the success of many theoretical works. To further illustrate this let us compare the F(1s)

binding energies relative to the C(1s) in both experiment and calculations. From the data reported above it is clear that the two F(1s) peaks in the experiments of Calatayud et al. appear at 399.4 and 403.4 eV relative to C(1s) respectively. Taking the average of the two calculated C(1s) values for the adsorbed trifluoroacetate (270.3 eV) as origin one would find the F(1s) features at 384.7 and 387.2 eV. The agreement now is semiquantitative and the difference between experimental and calculated values can be safely ascribed to final state effects. To conclude, the present theoretical calculations fully confirm the experimental assignment. The present discussion also validates and reinforces previous conclusions regarding the validity of Kohn-Sham orbital energies to predict relative values of core level binding energies.

Conclusions

Periodic density functional theory based calculations, with the PBE flavor for the exchange correlation functional, have been carried out to investigate the adsorption of TFAA on the anatase TiO_2(101) and TiO_2(001) surfaces. The analysis of the bonding modes and the results regarding the strength of the interaction reveal that TFAA adsorbs molecularly on the TiO_2(101) surface, the structure of the adsorbed molecule largely resembles that of the gas phase species and the small calculated value of the adsorption energy points towards a weak interaction. The opposite holds for the interaction of the TFAA molecule with the TiO_2(001) surface, the molecule dissociates into trifluoracetate and a proton, the trifluoroacetate moiety strongly binds to the surface in a bridging configuration and the proton binds to a nearby surface oxygen atoms that is considerably displaced towards the vacuum. The bonding mode is in agreement with suggestions from experiments regarding the TFAA mediated solvothermal synthesis of TiO_2 nanoparticles although these were unable to distinguish between the two surfaces. The present results fully justify the fact that TFAA stabilizes the more reactive TiO_2(001) surfaces. This comes simply from the much larger adsorption energy of TFAA on TiO_2(001). Therefore, once a small surface area is available for adsorption, TFAA will strongly adsorb thus hindering the growth of the most thermodynamically favored TiO_2(101). For the case of TFAA on the TiO_2(001) surface, analysis of the F(1s) core level binding energy confirms the experimental assignment of the low energy peak to F adsorbed at the surface as F^- and of the high energy peak to the F atoms in the $–CF_3$ group. Overall, the present paper contributes to understand the role of TFAA in directing the growth of TiO_2 particles with abundant (001) facets.

Acknowledgements

This work has been supported by the Spanish MINECO grant CTQ2012-30751 grant and, in part, by *Generalitat de Catalunya* grants 2014SGR97 and XRQTC. O.L.G is grateful to the *Universitat de Barcelona* for a predoctoral grant. Computational time at the MARENOSTRUM supercomputer has been provided by the Barcelona Supercomputing Centre through grants from *Red Española de Supercomputación* and the DSUNCAT project of the Partnership for Advanced Computing in Europe (PRACE).

Table 1.- Structural parameters of the isolated TFAA molecule as predicted from the present PBE calculations; results from previous work are included for comparison. The last row reports result for TFAA adsorbed on the TiO_2(001) surface in the most stable configuration. Distances are in Å and the F-C-F bond angle in degrees.

	C-F	C-F[a]	O-H	C-O	C=O	F-C-F[b]
Gas phase TFAA						
B3LYP/6-311+G(d,p)[55]	1.34	1.33	0.97	1.34	1.20	108
MP2(full)/6-311+G(d,p)[55]	1.34	1.33	0.97	1.34	1.21	108
PBE present work	1.34	1.37	0.98	1.35	1.20	109
Experimental[54]	1.32	1.32	0.96	1.35	1.19	109
Adsorbed TFAA						
PBE present work	1.35	1.36	0.98*	1.29	1.25	108

*) Note that TFAA chemisorbs dissociatively, this value corresponds to the distance between H and the O atom of the surface to which it is bonded.
a) F atom located at the COOH plane
b) Angle involving two symmetrically equivalent F atoms

Figure 1.- Slab models used to represent the anatase $TiO_2(001)$ and $TiO_2(101)$ surfaces; left and right panels, respectively. Ti atoms are in grey and O atoms in red. The atomic layers relaxed or fixed in the study of TFAA adsorption are also indicated.

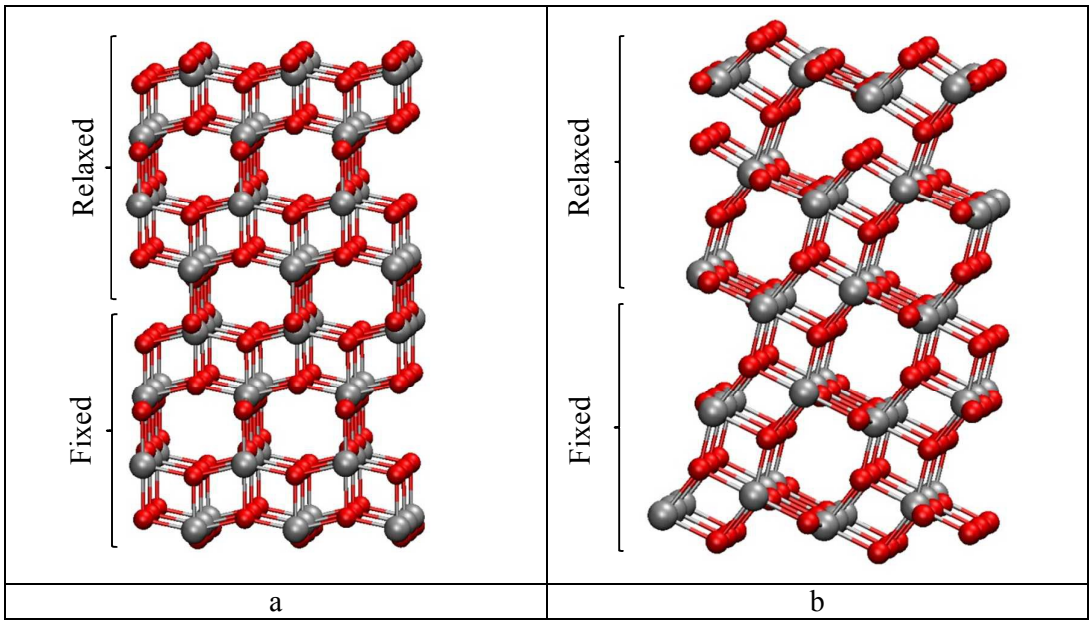

Figure 2.- Illustrative examples of chelating (a), bridging (b) and top (c) bonding modes of TFAA above the anatase TiO_2(001) surface.

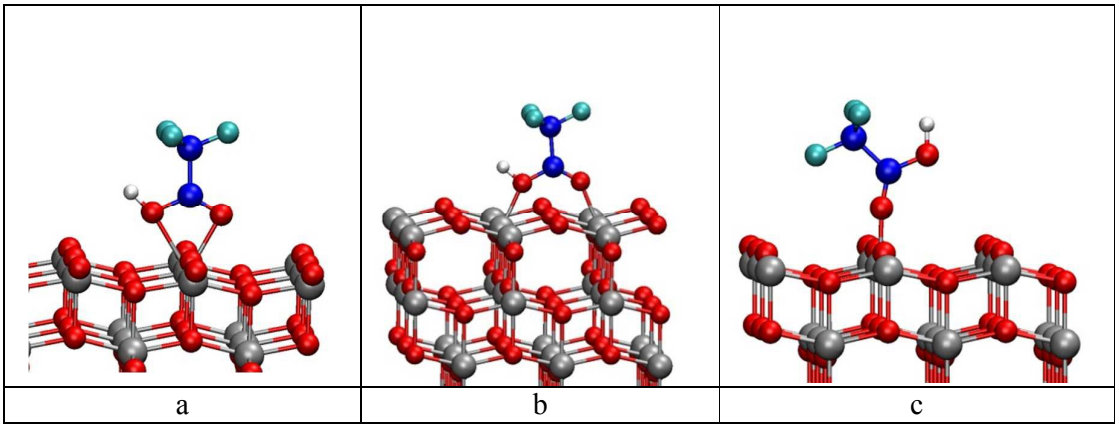

a b c

Figure 3.- Structure of the two most stable bonding modes and TFAA adsorbed on anatase TiO_2(101). Note that the TFAA molecule is adsorbed in a non-dissociative way.

Mode 1 (H-O_{surf})	Mode 2 (O-Ti_{surf})
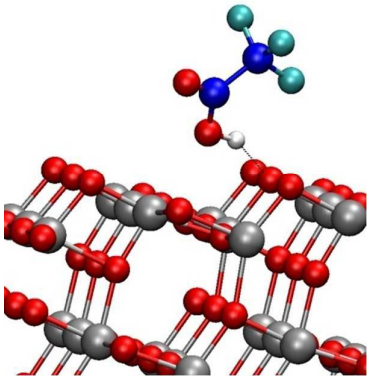	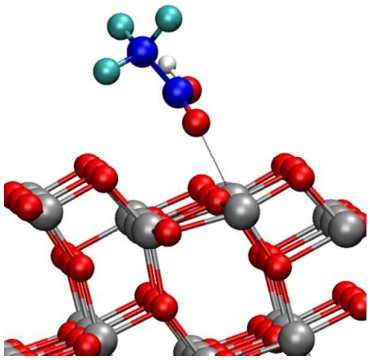

Figure 4.- Structure of the most stable bonding modes and TFAA adsorbed on anatase TiO_2(001). Note that here the TFAA molecule is adsorbed in dissociative way.

Side view	Front view
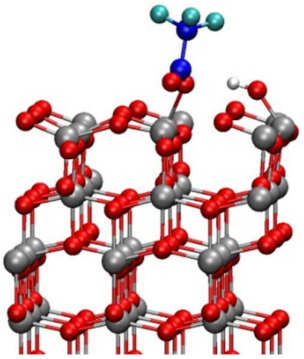	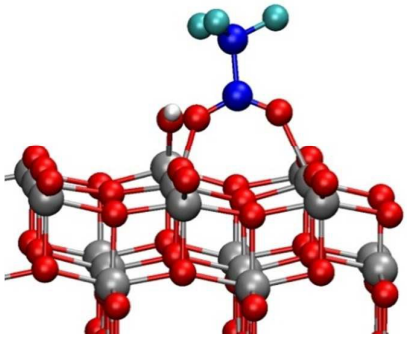

References

[1] M. R. Bahnemann, S. T. Hoffmann, W. Y. Martin, D. W. Choi, *Chem. Rev*. 1995, 95, 69.

[2] X. Chen, S. S. Mao. *Chem. Rev*., 2007, 107, 2891.

[3] X. Chen, S. Shen, L. Guo, S. S. Mao. *Chem. Rev*. 2010, 110, 6503.

[4] M. Ni, M. K. H. Leung, D. Y. C. Leung, K. Sumathy. *Renew. Sust. Energ. Rev.*, 2007, 11, 401.

[5] Y. Paz, Z. Luo, L. Rabenberg, A. Heller. *J. Mat. Res*., 1995, 10, 2842.

[6] K. P. Kuhn, I. F. Chaberny, K. Massholder, M. Stickler, V. W. Benz, H. G. Sonntag, L. Erdinger. *Chemosphere,* 2003, 53, 71.

[7] H. Chen, C. E. Nanayakkara, V. H. Grassian. *Chem. Rev.,* 2012, 112, 5919.

[8] A. Fujishima, X. Zhang, D.A. Tryk, *Surf. Sci. Rep*., 2008, *63* 515.

[9] K. Hashimoto, H. Irie, A. Fujishima, *Jpn. J. Appl. Phys*., 2005, *44*, 8269.

[10] B. Ohtani, O.O. Prieto-Mahaney, D. Li, R. Abe, *J. Photochem. Photobiol. A: Chem.,* 216 (2010) 179.

[11] C. di Valentin, G. Pacchioni. *Catal. Today*, 2013, 206, 12.

[12] L. Li, J. Yan, T. Wang, Z. Zhao, J. Zhang, J. Gong, N. Guan. *Nature Communications,* 2015. 6, 5881.

[13] R. Asahi, T. Morikawa, T. Ohwaki, K. Aoki, Y. Taga. *Science*, 2001, 293, 269.

[14] C. di Valentin, G. Pacchioni. *Acc. Chem. Res.,* 2014, 3233-3241.

[15] R. Asahi, T. Morikawa, H. Irie, T. Ohwaki. *Chem. Rev.*, 2014, 114, 9824.

[16] B. Ohtani..*Phys. Chem. Chem. Phys.,* 2014, 16, 1788.

[17] H. G. Yang, C. H. Sun, S. Z. Qiao, J. Zou, G. Liu, S. C. Smith, H. M. Cheng, G. Q Lu. *Nature*, 2008, 453, 638.

[18] F. Amano, T. Yasumoto, O. O. Prieto-Mahaney, S. Uchida, T. Shibayama, B. Ohtani. *Chem. Commun.,* 2009, 2311.

[19] F. Amano, T. Yasumoto, O. O. Prieto-Mahaney, S. Uchida, T. Shibayama, Y. Terada, B. Ohtani. *Top Catal.,* 2010, 53.

[20] G. Liu, H. G. Yang, J. Pan, Y. Q. Yang, G. Q. (Max) Lu, H. M. Cheng. *Chem. Rev.,* 2014, 114, 9559.

[21] Zhang, J.; Qian, L.; Yang, L.; Tao, X.; Su, K.; Wang, H.; Xi, J.; Ji,Z. *Appl. Surf. Sci.,* 2014, 311, 521.

[22] O. Lamiel-Garcia, S. Tosoni, F. Illas, *J. Phys. Chem. C*, 2014, 118, 13667.

[23] D. G. Calatayud, T. Jardiel, M.Peiteado, C. Fernández Rodríguez, M. R. Espino Estévez, J. M. Doña Rodríguez,F. J. Palomares, F. Rubio, D. Fernández-Hevia, A. C. Caballero. *J. Mat. Chem. A*, 2013, 1,14358.

[24] D. G. Calatayud, T. Jardiel, M. Rodríguez, M. Peiteado, D. Fernández-Hevia, A. C. Caballero, *Ceram. Int.,* 2013, 39, 1195.

[25] P. E. Blöchl, *Phys. Rev. B* 1994, 50, 17953.

[26] G. Kresse,J. Joubert, *Phys. Rev. B*, 1999, 59, 1758.

[27] H. I. Monkhorst, J. D. Pack, *Phys. Rev. B: Solid State*, 1976, 13, 5188.

[28] J. P. Perdew, J. A. Chevary, S. H. Vosko, K. A. Jackson, M. R. Pederson, D. J. Singh, C. Fiolhais, *Phys. Rev. B,* 1992, 46, 6671.

[29] J.P. Perdew, K. Burke, M. Ernzerhof, *Phys. Rev. Lett.,* 1996, 77, 3865.

[30] C. Sousa, S. Tosoni, F.Illas, *Chem. Rev.,* 2013, 113, 4456.

[31] H. Y. Lee, S. J. Clark, J. Robertson, *Phys. Rev. B,* 2012, 86, 075209.

[32] C. di Valentin, G. Pacchioni, *Catal. Today,* 2013, 206, 12.

[33] I. de P. R. Moreira, F. Illas, R.L. Martin, *Phys. Rev. B,* 2002, 65, 155102.

[34] G. Pacchioni, *J. Chem. Phys.* 2008, 128, 2008, 182505.

[35] E. Finazzi, C. di Valentin, G. Pacchioni, A. Selloni, *J. Chem. Phys.* 2008, 129, 154113.

[36] A. Janotti, J. B. Varley, P. Rinke, N. Umezawa, G. Kresse, C.G. Van de Walle, *Phys Rev. B,* 2010, 81, 085212.

[37] G. Kresse, J. Hafner, *Phys. Rev. B: Condens. Matter,* 1993, 47, 558.

[38] G. Kresse, J. Furthmuller, *Comput. Mater. Sci.* 1996, 6, 15.

[39] G. Kresse, J. Furthmuller, *Phys. Rev. B: Condens. Matter,* 1996, 54, 11169.

[40] J. K. Burdett, T. Hughbanks, G. J. Miller Jr., J. W. Richardson, J. V. Smith, *J. Am. Chem. Soc.,* 1987, 109, 3639.

[41] Y. Ortega, O. Lamiel-Garcia, D. Fernandez Hevia, S. Tosoni, J. Oviedo, M. A. San-Miguel, F. Illas, *Surf. Sci.*, 2013, 618, 154.

[42] Y. Liang, S. Gan, S. A. Chambers, E. I. Altman, *Phys. Rev. B* 2001, 63, 235402

[43] Y. Wang, H. Sun, S. Tan, H. Feng, Z. Cheng, J. Zhao, A. Zhao, B. Wang, Y. Luo, J. Yang, J. G. Hou, *Nature Comm.* 2013, 4, 2214

[44] F. Ito, *Chem. Phys.* 2011, 382, 52-57.

[45] F. Ito, *Comput. Theor. Chem.* 2013, 1016, 48.

[46] P. Krishnakumar, D. K. Maity, *J. Phys. Chem. A* 2014, 118, 5443

[47] W. Kun Li, X.Qing Gong, G. Lu, A. Selloni, *J. Phys. Chem C* 2008, 112, 6594

[48] K. L. Miller, J. L. Falconer, J. W. Medlin, *J. Catal.* 2011, 278, 321

[49] C. di Valentin, D. Fittipaldi, *J. Phys. Chem. Lett.* 2013, 4, 1901

[50] N. Pueyo Bellafont, F. Illas, P. S. Bagus. *Phys. Chem. Chem. Phys.*, 2015, 17 4015.

[51] N. Pueyo Bellafont, P. S. Bagus, F. Illas. *J. Chem. Phys.,* 2015, 142, 214102.

[52] L. Köhler, G. Kresse, *Phys. Rev. B*, 2004, 70, 165405.

[53] M. Happel, N. Luckas, F. Viñes, M. Sobota, M. Laurin, A.Görling, J. Libuda. *J. Phys. Chem. C*, 2011, 115, 479.

[54] Handbook of Chemistry and Physics, 84th Ed., edited by *D. R. Lide CRC, Boca Raton*, 2003. Section 9-40.

[55] M. Namazian, M. Zakery, M.R. Noorbala, M.L. Coote, *Chem. Phys. Lett.*, 451, 2008, 163.

[56] J. P. Prates Ramalho and F. Illas. *Chem. Phys. Lett.*, 2012, 545, 60.

[57] J. P. Prates Ramalho, J. R. B. Gomes, F. Illas. *RSC Adv., 3,* 2013, 13085.

[58] P.S. Bagus, F. Illas, G. Pacchioni, F. Parmigiani, *J. Electr. Spectrosc.Relat.Phenom.*, 1999, 100, 215.

[59] P. S. Bagus, E.S. Ilton, C. J. Nelin, *Surf. Sci. Reports,* 2013, 68, 273.

[60] A. A. Bakke, H. W. Chen, W. L. Jolly, *J. Electron. Spectrosc.& Rel. Phenom.*, 1980, 20, 333.